Auralization of Unsteady Rotor Noise using a Solution to the Ffowcs Williams-Hawkings Equation

Siddhartha Krishnamurthy
Structural Acoustics Branch
NASA Langley Research Center
Hampton, VA, USA

Brian C. Tuttle
Analytical Mechanics Associates, Inc.
Hampton, VA, USA

Stephen A. Rizzi
Aeroacoustics Branch
NASA Langley Research Center
Hampton, VA, USA

ABSTRACT

Auralization of unsteady helicopter flight operations is needed to better understand the impact of maneuvers on community noise. Previous source sound synthesis methods were based on interpolated data, which may lead to artifacts in generating sound for helicopter maneuvers where sound pressure directivity may change rapidly. In this paper, the source sound is synthesized at every time sample using a solution to the Ffowcs Williams-Hawkings Equation along the path of the emission angle between the source and a ground observer. The synthesized sound is then propagated to the ground observer for auralization. Since no interpolation is performed, maneuvers with rapidly changing sound pressure directivities may be more accurately synthesized and auralized. The framework for accomplishing this synthesis and auralization is described, which couples the Fundamental Rotorcraft Acoustic Modeling from Experiments, the second-generation Aircraft NOise Prediction Program, and the NASA Auralization Framework. Synthesis of a hovering rotor is presented to compare with previous synthesis methods. Two examples with aperiodic signals are then presented to demonstrate synthesis and auralization of unsteady rotor noise.

INTRODUCTION

Noise remains a significant challenge for increasing helicopter use among the public [1] [2] [3]. In addition to low-noise helicopter designs, improved understanding of how flight operations affect communities is needed. This paper is directed at a new capability to auralize rotorcraft flight maneuvers for the purpose of understanding human response to the noise they generate. Auralization is a technique for creating audible sound files from numerical data [4]. Here, it refers to the combined process of source noise generation and propagation to a ground observer. Auralizations can be played to human test subjects in the NASA Langley Exterior Effects Room (EER) [5] to assess the noise impact of rotorcraft maneuvers.

The maneuvering of helicopters involving accelerations and turning causes unsteady (aperiodic) blade pressures that can produce significantly more noise than straight and level flight. It is important to understand the impact of these rotorcraft maneuvers on community noise. The unsteady flight operations for this paper occur on timescales of at least several seconds. One example is the occurrence of increased blade-vortex-interaction noise that can happen when helicopters deviate from a straight and level flight, especially during aggressive maneuvers [6].

A helicopter auralization can be divided into two general steps: sound pressure synthesis and propagation. The synthesis process generates pressures at a helicopter, or source, before propagation to a ground observer. Prediction of the synthesized pressures can originate from various methods. One example is computational fluid dynamics (CFD) simulations. Another example is data on helicopter rotor geometry and aerodynamics, including blade loadings, from which sound pressure can be calculated using solutions to the Ffowcs Williams-Hawkings (FW-H) equation [7]. Blade loadings refer to forces, such as lift and drag, applied to rotor blades. The synthesized sound pressures are usually predicted at points on a hemisphere at some radial distance from the source [8] [9] [10] [11]. Propagation effects, such as atmospheric absorption and Doppler, are subsequently added to the synthesized sound to obtain the auralized sound at the ground observer.

Previous rotorcraft auralizations were of rotorcraft with straight and level flight paths. To produce straight and level flight, Ref. [8] assumed flight conditions for an AS350 helicopter to be steady and the sound pressure from the helicopter to be periodic. Steady flight conditions refer to rotorcraft control settings being maintained. In unsteady flight, where control settings change, aperiodic sound pressure signals are produced. Aperiodic signals can still be present in straight and level flight such as in the auralizations of an AS350 helicopter in Ref. [9] and a DJI Phantom 2 Quadcopter in Refs. [10] and [11]. For these auralizations, short duration aperiodic fluctuations were caused by rapid control changes needed to maintain level flight in the presence of, for example, turbulence. These auralizations did not include maneuvers involving accelerations and turning.

Presented at the Vertical Flight Society (VFS) 75th Annual Forum & Technology Display, May 13-16, 2019, Philadelphia, PA, USA.

In the process of auralizing helicopter maneuvers, a unique contribution of this paper is to compute noise on a hemisphere around the source only at points corresponding to the instantaneous emission angles between the source and the receiver. In previous auralizations, sound was synthesized on the source hemisphere at a discrete set of regularly spaced emission angles. The source sound at intermediate emission angles was computed by interpolation [8] [10] [11] [9]. In this paper, the source noise is directly computed at the instantaneous emission angle at each sampling instant, with no interpolation.

Previous auralization methods used the Comprehensive Analytical Rotorcraft Model of Rotorcraft Aerodynamics and Dynamics (CAMRAD II) [12] program to determine blade loadings and the second generation Aircraft NOise Prediction Program (ANOPP2) [13] to compute sound pressures on the source hemisphere. The NASA Auralization Framework (NAF) [14] was then used to propagate the source sounds to an observer to complete the auralization. This paper replaces CAMRAD II with the Fundamental Rotorcraft Acoustic Modeling from Experiments (FRAME) program [15] to generate rotor blade and aerodynamics data. FRAME can predict aperiodic forces on blades due to unsteady flight operations as well as blade loadings due to steady flight.

Three synthesis and auralization examples are presented in this paper. The first example compares the new synthesis approach of this paper with the previous synthesis method involving interpolation between discrete emission angles. Comparison of these methods uses the steady flight condition of a hovering rotor at a range of source emission angles corresponding to a moving ground observer. The second example demonstrates that unsteady flight operations can be auralized for long durations using a straight and level flyover as simple proof-of-concept. The last example is a shorter duration auralization where the rotor experiences unsteady maneuvers involving accelerations.

SYNTHESIS

Helicopter Flyover Overview

To setup a helicopter flyover auralization, paths for the helicopter and ground observer are specified as a function of time. The vehicle spatial position (x,y,z) with respect to the origin, and its attitude (heading, roll, pitch) define the flight path. Likewise, the ground observer can also follow a path with changing spatial coordinates relative to the helicopter, although the observer is typically stationary.

Along with the flight and observer paths, sound propagates along a path at each time instant with an emission angle from the helicopter to the ground observer. For this work as well as in Ref. [8], sound from a particular emission angle is computed using Farassat's formulation 1A (F1A), which is a solution to the FW-H equation [7] [16]. Rotor geometry and blade loadings serve as input to the sound prediction calculations.

The predicted sound can be either periodic or aperiodic. If it is periodic, typically only a single blade passage or a single rotor revolution of helicopter sound pressure is predicted using F1A at a particular emission angle. From these short duration pressure signals, the periodic signals can subsequently be extended indefinitely in time at the emission angle. If the predicted sound is aperiodic, the sound pressure for the full duration of the auralization must be computed using F1A.

Synthesis with Interpolation

Figure 1 depicts the method of synthesis used for previous auralizations of moving rotorcraft [8] [10] [11] [9]. Here, the F1A method is used to calculate sound pressures at discrete spatial points on a source hemisphere around the rotorcraft. The hemisphere mesh represents the discretization. As the rotorcraft moves over the observer, the emission angle to the observer varies between discrete emission angles on the source hemisphere.

To propagate these periodic source sound pressures to an observer, the NAF implements a method called periodic sound synthesis to calculate the sound pressure at intermediate emission angles [14]. This method decomposes the predicted blade passage signals at the discrete emission angles into harmonics of the blade passage frequency (BPF) and extracts their magnitude and phase. It then interpolates those quantities at intermediate angles. An additive synthesis technique is then applied to the interpolated harmonic magnitudes and phases to generate sound pressure as the emission angle changes. Ref. [8] and [10] describe the interpolation process in more detail.

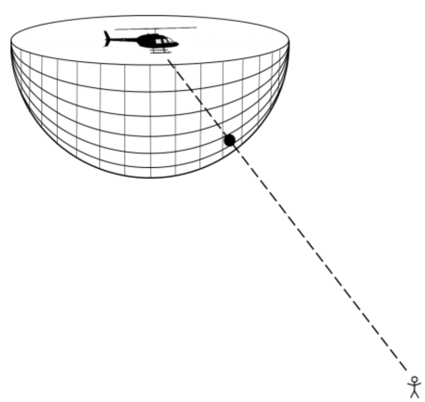

Figure 1. Previous method of synthesizing sound pressures.

Synthesis with interpolation has certain drawbacks. One drawback is that an insufficiently refined discretization of the source hemisphere relative to the source directivity can result in artifacts in the auralization. Using a finer discretization may be limited by computational capabilities such as available memory. Another drawback is that synthesizing aperiodic signals using interpolation becomes more challenging. Depending on the characteristics of the aperiodic signals at the discrete emission angles, it may not be clear how to interpolate the sounds at the intermediate angles. Ref. [9] interpolated aperiodic signals in straight and level flight by modeling amplitude fluctuations as bandlimited random processes and using an overlap-add technique. In Ref. [10], pink noise was directly added to the synthesized sounds. These methods produced aperiodic fluctuations of short duration but do not extend to synthesizing the long duration unsteady flight operations in this work.

Synthesis with Direct Computation of Sound Pressures

Figure 2 illustrates the new synthesis method for synthesizing unsteady flight operations. Here, F1A is used to compute the source noise at each time sample at the instantaneous emission angle between the source and the ground observer. A single point on the hemisphere at the emission angle to the observer follows a track along the hemisphere as the rotorcraft flies over the observer. This point and its track form the "Tracking Observer." As this source point is determined at each sample instant, the result is a much finer discretization of the source hemisphere without interpolation. In this manner, only source points that propagate to the observer are calculated, not other points over the hemisphere. This synthesis approach is referred to as "F1A Synthesis." Both periodic and aperiodic signals may be computed with F1A synthesis.

AURALIZATION FRAMEWORK

Figure 3 shows the coupling of the computational components needed for auralization of flight operations using the F1A Synthesis approach.

Blade Loadings: FRAME

The left side of the flowchart shows FRAME, the primary objective of which is to provide rotor blade data for sound pressure predictions. FRAME provides a semiempirical model of helicopter noise generation. Inputs to FRAME are blade geometry and motion, as well as rotor trajectory. These input parameters define the flight operation. FRAME's model is based on either flyover or wind tunnel rotor acoustical measurements. It can also come from aerodynamic predictions if measurements are not available. FRAME segments each blade and outputs data for each segment, as shown in Figure 4. The solid black line in Figure 4 through the blade represents a segmented compact-line-source, which the source noise prediction after FRAME approximates as the blade geometry. The source noise prediction requires the following time-dependent output from FRAME: blade loadings including drag and lift coefficients and blade geometry parameters such as area prior to the compact-line-source approximation. The sampling rate used by FRAME is approximately 5 kHz. Hence, the sound pressures predicted from FRAME data implicitly assume that the contributions of frequencies greater than 2.5 kHz are negligible. FRAME output depends on whether the data are used to compute periodic or aperiodic sound pressures. If periodic, the FRAME data are a blade passage or rotor revolution in duration. If aperiodic, the FRAME data will be as long as needed by the auralization. Refs. [6] and [15] provide additional details on FRAME.

Emission Angles: NAF Path Finder

The right side of the flowchart in Figure 3 shows the NAF Path Finder [14]. Its purpose is to generate tracking observer positions along the source hemisphere. Using flight path information, the Path Finder computes the azimuthal and polar emission angle to the ground observer for each time step in the auralization, assuming a straight-line propagation path. The flight path data include the rectangular coordinates, x, y, and z, and the vehicle's attitude (heading, pitch, and roll). These flight path data can be determined from the rotor and flight trajectory provided by the user. It can also come from tracking data obtained through helicopter flyover measurements if the user wishes to auralize a previously recorded flyover. Ground observer position is also provided to the Path Finder by the user. The emission angle is then transformed to the source frame of reference. This transformation ensures that changes in heading, pitch, and roll will cause a change in emission angle, even if the source position is fixed. The tracking observer position is subsequently calculated using the emission angle and the tracking hemisphere radius. The tracking observer positions are output as a time series with a sampling rate that matches the FRAME sampling rate.

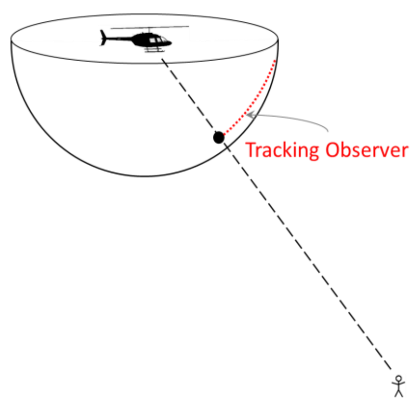

Figure 2. Synthesis method of directly computing sound pressures at each time sample.

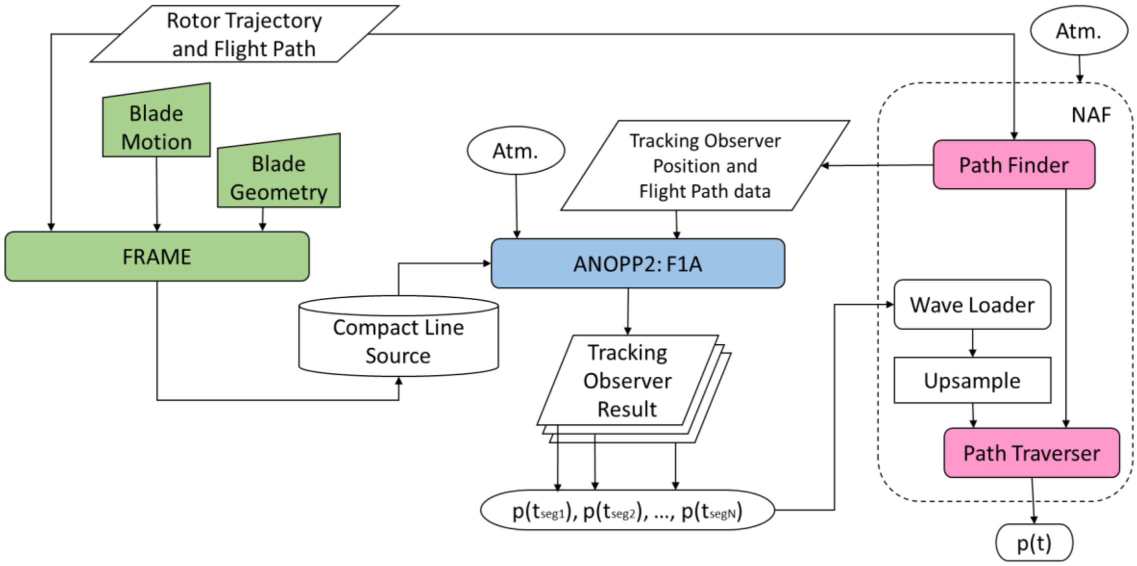

Figure 3. Flowchart for F1A Synthesis and Auralization.

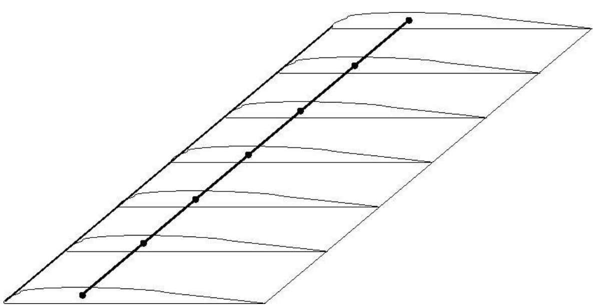

Figure 4. Segmented blade and compact-line-source.

Sound Synthesis: ANOPP2

ANOPP2 uses its F1A solver to calculate the sound pressure at each point along the tracking observer [13]. To run the calculation, it reads in the data from FRAME and the tracking observer positions from the NAF Path Finder. The tracking observer positions from the NAF Path Finder tell ANOPP2 at which directivity angle to compute the sound pressures. The total computed sound pressure is a sum of the loading and the thickness pressures, which are both calculated by ANOPP2. Drag and lift coefficients in the FRAME output are used by ANOPP2 to calculate loading pressure, and blade geometry from FRAME is used to calculate thickness pressure. ANOPP2 computes the total sound pressure at the same rate as FRAME, approximately 5 kHz.

ANOPP2 uses both the far-field ($1/r$) and near-field ($1/r^2$) terms of the thickness and loading noise components of its F1A solver, where r is the radial distance from source to observer (See Eqs. 67 and 68 of Ref. [17]). To propagate the output of ANOPP2 to a ground observer, the NAF requires a far-field propagating solution, but the ability to remove the near-field terms does not exist in the current version of ANOPP2. To reduce the contribution of the near-field terms, sound pressures were synthesized using F1A at radii significantly larger than the rotor radii. This approach also eliminates the zero-frequency offset caused by hydrostatic pressure associated with the downwash from the rotor in the acoustic pressure calculation. The synthesized pressures are then scaled to a one-meter reference distance to account for spreading loss in the far-field terms. A time shift is also applied to remove the propagation delay from the rotor to the far-field observer. Propagation delay is computed for a constant speed of sound resulting from specification of a uniform atmosphere. No other atmospheric effects, e.g., atmospheric absorption, are included in the F1A synthesis.

The synthesized sound pressure computed in ANOPP2 is dependent on whether the pressure is to be periodic or aperiodic. ANOPP2 approximates the rotor blade as a segmented compact-line-source as was shown and discussed previously with Figure 4. The time for each segment of the compact-line-source rotor blade to propagate its contribution to the tracking observer will be different. The first sound pressure reading at the tracking observer with contributions from all rotor segments is delayed, where the delay is based on the difference in propagation times between the nearest and farthest rotor segments. For periodic sound pressures, however, a delay will not exist. When the FRAME data specify that sound pressures are periodic, ANOPP2 assumes that the data are known for all time, even negative time for the emission time corresponding to the most distant line source element.

In Figure 3, the output of ANOPP2 shows multiple layers of the tracking observer result. If the synthesized sound duration exceeds computer memory constraints, the maneuver simulation time is broken up into multiple segments. The

F1A calculation for each segment is performed separately, and the segments are then later joined together. Each layer in the ANOPP2 output in Figure 3 represents a different predicted sound pressure segment. ANOPP2 maintains the source motion over adjacent segments to produce the correct signal phase at segment boundaries.

Propagation: NAF Path Traverser

The NAF Path Traverser propagates the F1A synthesis result from ANOPP2 to a ground observer. As shown on the right side of Figure 3, the NAF reads the sound pressure segments from the F1A synthesis and then concatenates and upsamples them using a polyphase filter to 44.1 kHz. The Path Traverser combines the upsampled synthesized signal with the Path Finder emission angle calculations and propagates the synthesized sound to a ground observer to complete the auralization. Propagation effects including absolute delay, spreading loss, atmospheric absorption, and ground plane reflections are generally included in the NAF propagation. The change in absolute delay over time simulates Doppler shift.

Path Traverser Buffer Size

The spreading loss, absolute time delay, and atmospheric absorption are determined in the NAF Path Traverser [14] on a buffer (or hop) size of n samples (typically 512), corresponding to a time interval (typically 11ms) at the audio sampling rate of 44.1 kHz. These are cast in terms of a negative gain (G), time delay (T), and filter (F). Propagation occurs in the NAF GTF engine, which linearly interpolates and applies the G, T, and F to each sample in the block. If the motion of the source is such that the interpolated values significantly deviate from the actual values, then the buffer size should be reduced. This can occur for a straight and level steady flight, and may be exacerbated for a maneuvering flight (next section). No attempt was made to quantify such differences in this work; it was assumed that the 512 buffer size was sufficient. However, this aspect of the propagation processing is worthy of future consideration.

Process Extension

Although the F1A synthesis and auralization process explained in this paper targets helicopter rotors, it can be applied to any propeller or rotor with blade pressures and motions in the form of a compact line source. In principal, noncompact sources such as blade pressures from CFD solutions can also be used. However, doing so will require further attention to memory management.

EXAMPLE 1: SYNTHESIS OF HOVERING ROTOR

In this first example, a hovering rotor is used to compare F1A synthesis with the previous synthesis method involving interpolation. The hover operating condition was specified using periodic data from FRAME based on aerodynamic predictions of a YHO-2HU helicopter rotor in hover. This rotor consisted of three blades with a rotor radius of 5.4 meters and BPF of 22.6020 Hz.

To exercise the tracking observer computations, a ground observer is assumed to be moving at a constant velocity of 26 m/s along a straight path 150 meters below the hovering source. The solid black trace in Figure 5 shows the time history of the emission angle computed by the NAF Path Finder from the stationary rotor to the ground observer. The azimuthal or lateral angle was set to $\phi = 0$ degrees so that travel was along the rotor centerline. The time history of the tracking observer positions had a sampling rate of 5.4245 kHz.

With the rotor data from FRAME and the tracking observer positions from the NAF, ANOPP2 performs the F1A synthesis at a radius of 1034.5 meters to minimize near-field terms and hydrostatic pressure offset. An inflow angle of 2.9 degrees and a coning angle of 6 degrees were assumed. Scaling and time shifting are then applied to generate sound pressures at a one-meter-reference distance. The blue trace in Figure 5 shows the resulting sound pressures at the tracking observer. Figure 6 and Figure 7 show the F1A Synthesis results for loading and thickness noise, respectively. These are comparable to the results published in Ref. [18] on pages 477-478 for a YHO-2HU helicopter in hover. The red, blue, and green traces represent each blade's contribution, and the black traces are the summed pressures from all the blades.

When studying the blue trace in Figure 5, it is apparent that lower pressures exist when the observer moves directly under the hovering rotor, when the emission angle is 90 degrees. With steady airloads, loading noise near the axis of rotation, which is directly under the rotor, is nearly zero. Further, thickness noise comes from steady sources so its pressure contribution directly under the rotor is minimal.

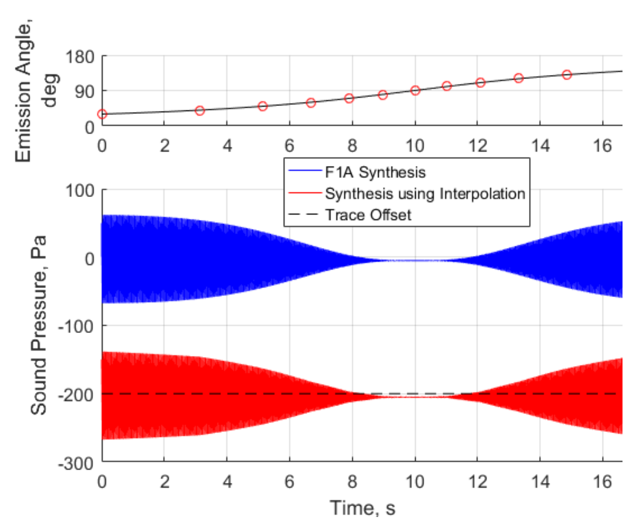

Figure 5. Synthesis of hovering compact line source rotor.

The red trace in Figure 5 was synthesized using the previous method by interpolating periodic data on a hemisphere between discrete emission angles. Since the azimuthal angle was zero degrees, a polar (front to back) discretization was used with angles ranging from 10 to 170 degree, in 10-degree increments. The red circles on the emission angle plot in Figure 5, starting at 30 degrees at time zero, represent the 10-degree separated angles between which periodic blade passage data were interpolated to generate the red trace.

To more clearly see the difference in the two synthesis results, the two synthesis traces are overlaid in Figure 8 for time between six and nine seconds. The time histories of both synthesis results match at the times corresponding to the discrete emission angles, shown by red circles, used to provide data for periodic synthesis with interpolation. Between these discrete angles, the time histories differ slightly, with the interpolated result having slightly higher power than the result from the tracking observer. Differences between the two methods might be greater if the source directionality were greater than in this example.

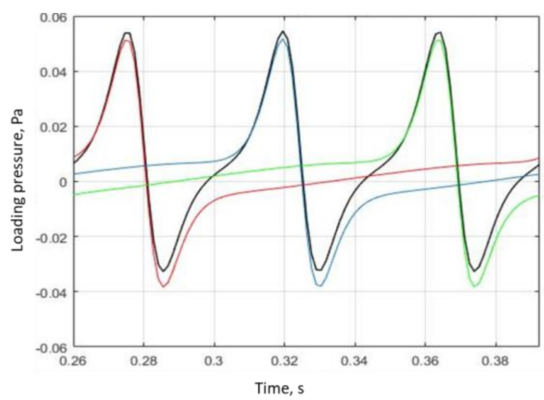

Figure 6. Loading pressure only from F1A Synthesis of acoustic data line rotor in hover.

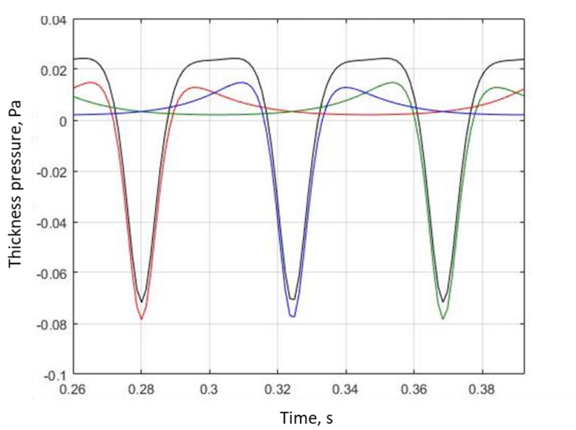

Figure 7. Thickness pressure only from F1A Synthesis of acoustic data line rotor in hover.

EXAMPLE 2: AURALIZATION WITH APERIODIC SOURCE

One benefit of the F1A synthesis method is the ability to more easily synthesize aperiodic data arising from unsteady operations than using interpolation methods. In this second example, a straight and level steady flight at constant velocity is used to demonstrate F1A synthesis of long duration aperiodic data.

Like the hovering case in the last example, straight and level steady flight produces periodic sound pressures. However, recall that FRAME can specify in its output whether the sound pressures to be synthesized are periodic or aperiodic. In this second example, the FRAME computation for a one minute long straight and level steady flight operation was changed by user input to treat the sound pressures as aperiodic. As a result, the FRAME output provided blade loadings for the entire duration of the auralization and not just the first rotor revolution. ANOPP2 treated the FRAME data as aperiodic with a start and a stop time instead of having indefinite duration.

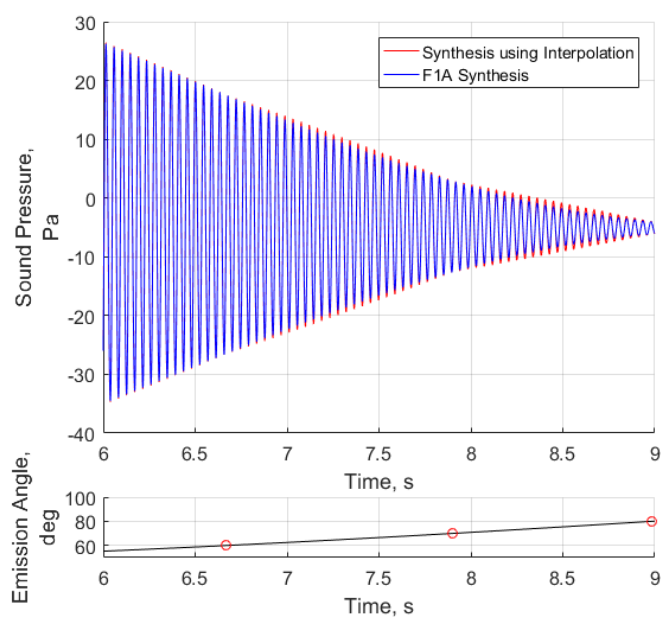

Figure 8. Comparing synthesis amplitudes.

Details of the flight setup and auralization are as follows. A rotor was flown at a constant velocity of 32 m/s at 150 meters above the ground for one minute. The rotor began its flight approximately one kilometer away from the ground observer. FRAME data for the rotor were again based on aerodynamic predictions of the YHO-2HU helicopter. A stationary sideline observer flush with the ground and approximately 412 meters perpendicular to the flight path was specified. Figure 9 illustrates the ground observer position with respect to the flight path. In this scenario, the NAF Path Traverser calculates the tracking observer at 70 degrees lateral to the rotor, that is, at an azimuthal emission angle of $\phi = 70$ degrees.

The F1A synthesis in ANOPP2 was executed similarly as for the hovering rotor. Tracking observer positions were read by ANOPP2 at a 5.5125 kHz rate. Synthesis occurred at a radius of 1034.5 meters before being scaled and time shifted to a one-meter reference distance. One notable difference from the hovering case was that the synthesis start time began 0.5 seconds after the beginning of the FRAME data. Since ANOPP2 regarded the data as aperiodic, sufficient delay had to be provided to allow contributions from all spatially distributed segments of the rotor to propagate to the observer for the first sound pressure reading. After obtaining the tracking observer result, the synthesized sound was then up-sampled in the NAF to 44.1 kHz for propagation. A standard uniform atmosphere was used in the propagation.

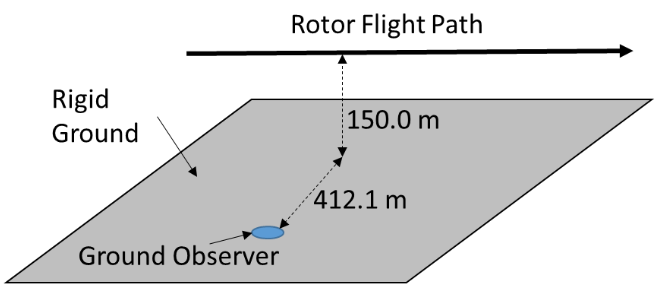

Figure 9. Illustration of ground observer distance from flight path (Not to scale).

Figure 10 shows the resulting auralized sound pressure time history at the ground observer. The black trace in Figure 10 shows the instantaneous elevation emission angle, which equals 90 degrees at 30 seconds into the flyover. The peak sound pressure occurs at 31.12 seconds. Accounting for propagation delay, the peak sound pressure was transmitted extremely close to the 90-degree emission angle. A delay of approximately three seconds appears at the beginning of the time history in Figure 10, corresponding to the propagation delay from the rotor's starting position one kilometer away from the ground observer. The auralized sound in Figure 10 can be found at Ref. [19]. Figure 11 gives a magnified view of the auralized time history where the signal oscillations can be seen.

The auralized result in Figure 10 and Figure 11 demonstrates that the F1A synthesis approach can be applied to aperiodic sources of long duration.

EXAMPLE 3: AURALIZATION WITH ACCELERATED SOURCE

Treating a steady flight operation as aperiodic data demonstrates how F1A synthesis can be used for unsteady operations. Now, in this third example, aperiodic data from an actual unsteady operation were generated in FRAME and synthesized using F1A for an accelerating rotor. Measured flight information from a Bell 206B helicopter with a two-blade rotor [6] was used by FRAME to generate data for a rotor in accelerated movement.

Figure 12 and Figure 13 show the rotor position and attitude time histories, respectively. Figure 14 shows the rotor position with respect to a stationary ground observer. All motion was in the x-z plane, and the azimuthal angle was $\phi = 0$ degrees.

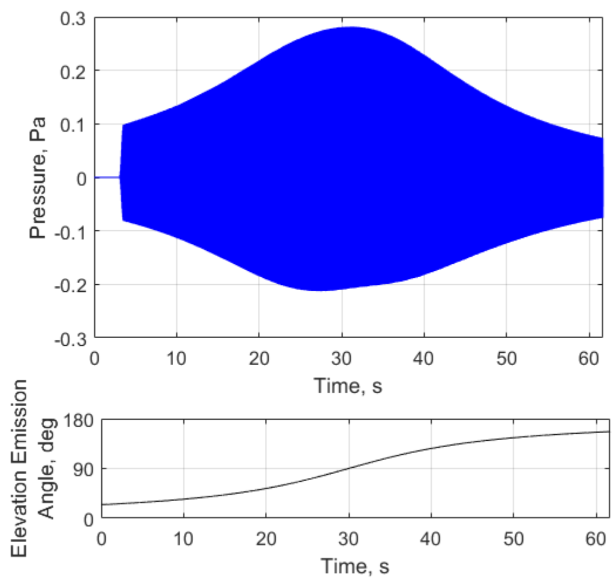

Figure 10. Auralized signal of F1A Synthesized aperiodic source.

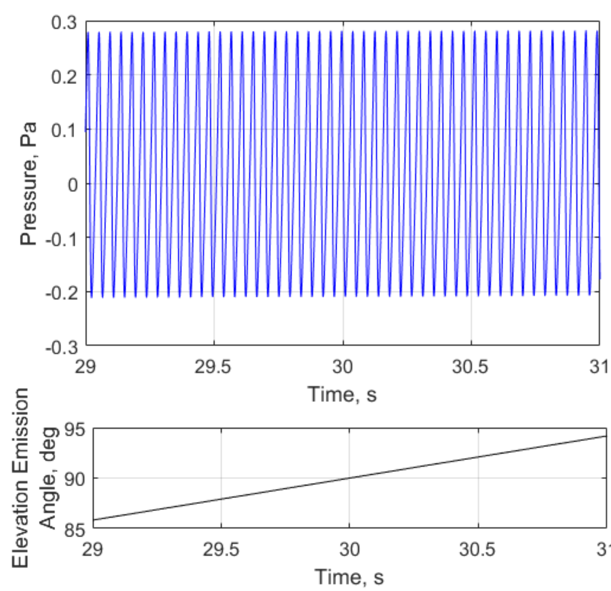

Figure 11. Magnified view of F1A Synthesized aperiodic source auralization time history.

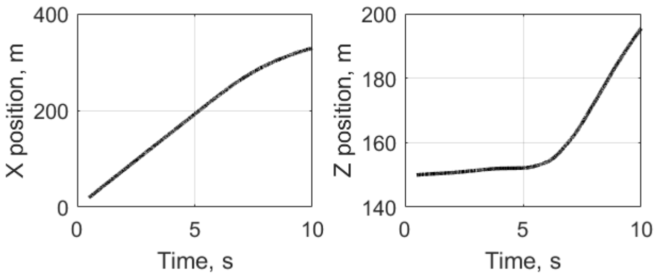

Figure 12. Accelerated rotor position time history.

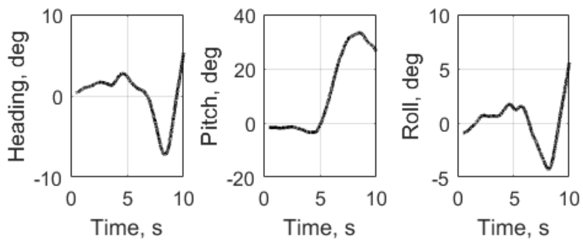

Figure 13. Accelerated rotor attitude time history.

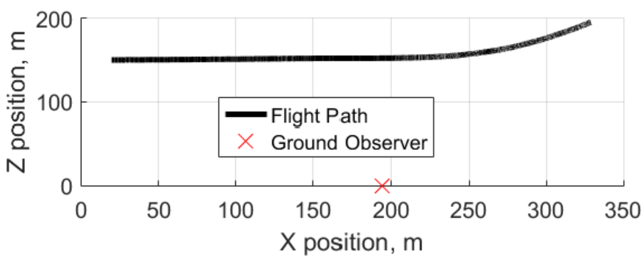

Figure 14. Accelerated rotor flight path with respect to ground observer.

The F1A synthesis for the rotor in unsteady flight proceeded similarly to the previous example. Figure 15 shows the auralized sound of the accelerating rotor after the NAF Path Traverser along with the emission angle at the source. A rigid ground and standard uniform atmosphere were used in the propagation. Along with the elevation emission angle, the azimuth emission angle is shown below the time history plot in Figure 15. Although the motion of the aircraft and ground observer location were all in the x-z plane, heading and rolling motion by the aircraft produced emissions to the ground observer in the azimuthal direction from the aircraft's frame of reference. The magnified view of the auralization time history in Figure 16 shows the shape of the signals. Here, the rotor produced blade-vortex interaction noise in its maneuver. A sound file for the auralization is available at Ref. [19].

CONCLUSIONS

A method for F1A synthesis and propagation for auralization of rotorcraft in maneuvering flight has been presented. Three examples are presented to demonstrate the coupling of FRAME, ANOPP2 and the NAF. The first example of a hovering rotor compares F1A synthesis with previous synthesis methods based on interpolation. The second example synthesizes and auralizes a rotor in steady operation, but its signal is considered aperiodic by ANOPP2 to demonstrate that F1A synthesis can be used for a long duration. The final example synthesizes and auralizes a rotor in accelerating flight. These examples demonstrate that F1A synthesis can be applied to auralize helicopter maneuvers to study their impact on community noise.

In Ref. [8], synthesizing a rotor flyover using interpolation produced artifacts especially near the middle of the flyover. Those artifacts were mitigated by finer discretization of the source hemisphere, but further discretization was limited by available memory required by the computational tools. The synthesis of the rotor in Ref. [8] can now be revisited in the near future using F1A synthesis.

Although FRAME is used to provide the rotor blade data for ANOPP2, it is only one of several options. CAMRAD-II [12] or the ANOPP Propeller Analysis System [20] may also provide input. Future work will focus on formalizing this approach into a NAF advanced plugin library to facilitate inclusion of data from these other sources.

Author contact: Siddhartha Krishnamurthy
siddhartha.krishnamurthy@nasa.gov,
Brian C. Tuttle brian.c.tuttle@nasa.gov,
Stephen A. Rizzi s.a.rizzi@nasa.gov.

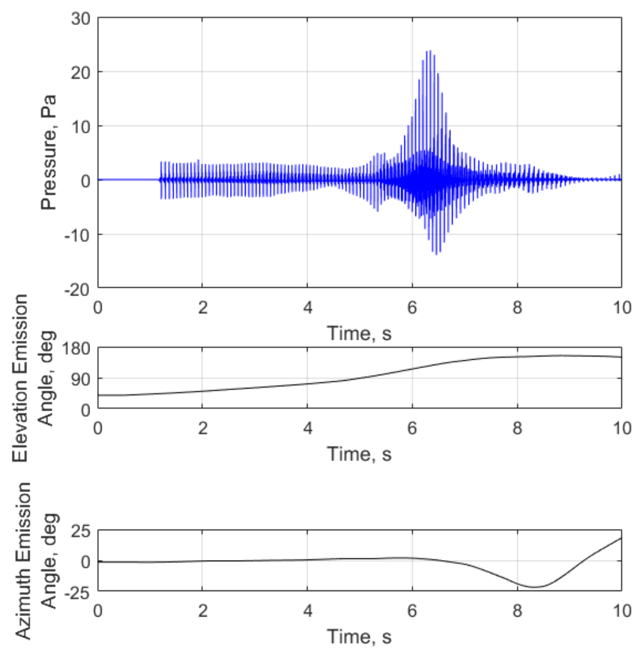

Figure 15. Auralized signal of F1A Synthesized rotor experiencing unsteady flight.

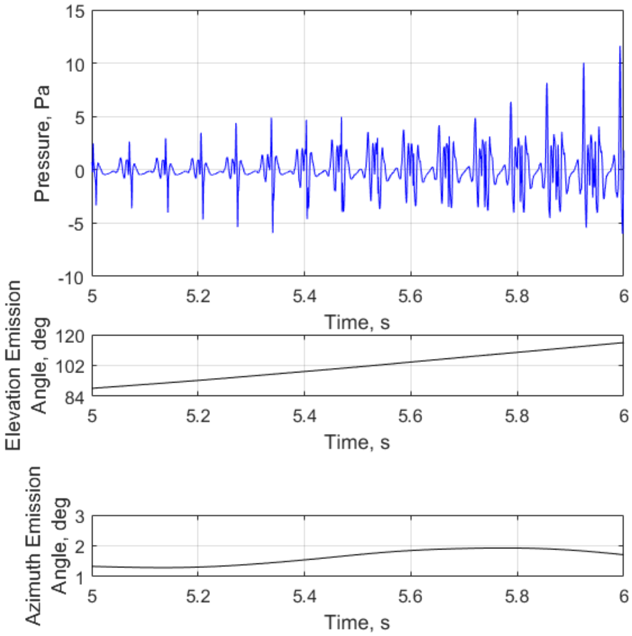

Figure 16. Magnified view for accelerating rotor auralization time history.

ACKNOWLEDGMENTS

This research was supported by the National Aeronautics and Space Administration, Aeronautics Research Mission Directorate, NASA Advanced Air Vehicles Program, Revolutionary Vertical Lift Technology Project.

REFERENCES

[1] "Report on the Los Angeles Helicopter Noise Initiative," Federal Aviation Administration, 2013.

[2] "The New York North Shore Helicopter Route, 14 CFR Part 93, Docket No. FAA-2010-0302," Federal Aviation Administration, Department of Transportation, 2010.

[3] T. R. Board, National Academies of Sciences and Medicine, *Assessing Community Annoyance of Helicopter Noise*, V. Mestre, S. Fidell, R. D. Horonjeff, P. Schomer, A. Hastings, B. G. Tabachnick and F. A. Schmitz, Eds., Washington, DC: The National Academies Press, 2017.

[4] M. Vorländer, *Auralization - Fundamentals of Acoustics, Modelling, Simulation, Algorithms and Acoustic Virtual Reality*, Springer-Verlag Berlin Heidelberg, 2008.

[5] K. J. Faller II, S. A. Rizzi and A. R. Aumann, "Acoustic performance of a real-time three-dimensional sound reproduction system," NASA/TM-2013-218004, Hampton, VA, 2013.

[6] E. Greenwood, F. H. Schmitz and R. D. Sickenberger, "A Semiempirical Noise Modeling Method for Helicopter Maneuvering Flight Operations," *Journal of the American Helicopter Society*, vol. 60, pp. 1-13, 2015.

[7] J. E. F. Williams and D. L. Hawkings, "Sound Generation by Turbulence and Surfaces in Arbitrary Motion," *Philosophical Transactions of the Royal Society of London. Series A, Mathematical and Physical Sciences*, vol. 264, pp. 321-342, 1969.

[8] S. Krishnamurthy, S. A. Rizzi, D. D. Boyd and A. R. Aumann, "Auralization of Rotorcraft Periodic Flyover Noise from Design Predictions," in Proceedings of the 74th Annual Forum, American Helicopter Society International, Phoenix, AZ, 2018.

[9] S. Krishnamurthy and S. A. Rizzi, "Auralization of Amplitude Modulated Helicopter Flyover Noise," in AIAA Scitech 2019 Forum, AIAA 2019-2087, San Diego, CA, 2019.

[10] A. Christian, D. D. Boyd, N. S. Zawodny and S. A. Rizzi, "Auralization of tonal rotor noise components of a quadcopter flyover," in InterNoise 2015, San Francisco, CA, USA, 2015.

[11] A. Christian and J. Lawrence, "Initial Development of a Quadcopter Simulation Environment for Auralization," in Proceedings of the 72nd Annual Forum, American Helicopter Society International, West Palm Beach, FL, 2016.

[12] W. Johnson, "Comprehensive Analytical Rotorcraft Model of Rotorcraft Aerodynamics and Dynamics, Version 4.10," in *Johnson Aeronautics, Volumes I-9*, 2017.

[13] L. V. Lopes and C. L. Burley, "ANOPP2 User's Manual," NASA/TM-2016-219342, Hampton, VA, 2016.

[14] A. R. Aumann, B. C. Tuttle, W. L. Chapin and S. A. Rizzi, "The NASA Auralization Framework and plugin

architecture," in InterNoise 2015, San Francisco, CA, USA, 2015.

[15] E. Greenwood, F. Schmitz and R. D. Sickenberger, "A Semi-Empirical Noise Modeling Method for Helicopter Maneuvering Flight Operations," in American Helicopter Society 68th Annual Forum, Fort Worth, TX, USA, 2012.

[16] F. Farassat and G. P. Succi, "The Prediction of Helicopter Rotor Discrete Frequency Noise," *Vertica,* vol. 7, pp. 309-320, 1983.

[17] F. Farassat, "Derivation of Formulations 1 and 1A of Farassat," NASA/TM-2007-214853, Hampton, VA, 2007.

[18] F. D. Harris, "Introduction To Autogyros, Helicopters, and Other V/STOL Aircraft," NASA/SP–2012-215959 Vol II, Ames Research Center, Moffett Field, California 94035-1000, 2012.

[19] "Aircraft flyover simulation," NASA, 2018. [Online]. Available: https://stabserv.larc.nasa.gov/flyover/.

[20] L. C. Nguyen and J. J. Kelly, "A Users Guide for the NASA ANOPP Propeller Analysis System," NASA Contractor Report 4768, Hampton, VA, 1997.